Water Supply

IWA PUBLISHING

Water Supply Vol 24 No 3, 707 doi: 10.2166/ws.2024.037

Effects of climate and land use change on runoff of the Second Songhua River Basin guided by SWAT model

Hongxue Liu [a,*], Jifa Liu[a] and Wanqiu Chen[a,b]

[a] Environmental and Social Development Research Center, Chang'an University, Xi'an 710061, China
[b] School of Materials Science and Engineering, Henan Institute of Technology, Xinxiang 453003, China
*Corresponding author. E-mail: 2018011001@chd.edu.cn

HL, 0000-0003-3794-3179

ABSTRACT

The driving effect of global climate change (CC) on the ecohydrological process was quantitatively evaluated. Based on Geographic Information System technology, a Soil and Water Assessment Tool model suitable for watershed hydrological simulation was constructed to study the impact of climate and land-use change on runoff in the Second Songhua River (SSR) basin. Within the base period (1965–2010), the annual average temperature (AAT) of the SSR basin is 4.2 °C. Under the CC scenario representing concentration pathway (RCP) 4.5, the AAT of the watershed increased to 5.4 °C between 2020 and 2049. Under the CC scenarios of RCP 8.5 and RCP 4.5, the temperature in the watershed increased by 1.1 and 0.2 °C in June, respectively. The research results indicate that (1) there is a positive correlation between runoff and precipitation in the SSR watershed, and a negative correlation with temperature; (2) when the precipitation remains unchanged, the temperature increases by 1 °C and the runoff decreases by 7.2%; and (3) when the temperature remains constant, for every 10% increase in precipitation, the runoff increases by 30.5%. This study provides the scientific basis for water resource planning and sustainable development in the Northeast region and has important practical significance.

Key words: climate, land use, runoff, SWAT model, Second Songhua River

HIGHLIGHTS

- Analyze the historical change characteristics of hydrometeorological elements.
- Establish the Soil and Water Assessment Tool model suitable for watershed hydrological simulation.
- Study the changes of hydrological elements in the basin under different land-use scenarios.

1. INTRODUCTION

Over the past 50 years, almost all regions worldwide have experienced global warming. From 1880 to 2012, the global temperature increased by 0.85 °C. Furthermore, global warming may have a significant influence on the hydrological cycle (Zhang *et al.* 2019a, 2019b; Yan *et al.* 2021). The variation in hydrological conditions and available water resources caused by climate change (CC) not only seriously affects the local ecology and socioeconomic development but also impacts the lower reaches. Therefore, understanding the spatiotemporal response of water resources to CC is crucial for determining future water use and formulating sustainable management plans. In recent years, the significance of assessing the impact of CC on river runoff has been increasingly recognized (Ma *et al.* 2019; Zhu *et al.* 2019; Kumar *et al.* 2023a, 2023b). Certain elements, including agrotype, topography, rainfall, infiltration, and vegetation, may affect surface hydrology and water usefulness. Consequently, distributed hydrological models and climate prediction data must be adopted to evaluate the potential impacts of CC on water resources.

The Songhua River is the main source of industries, ecosystems, public drinking water, and agriculture in northeast China. Thus, the CC and flow assessment of the river have become vital issues in the area (Anache *et al.* 2018; Berihun *et al.* 2019; Hu *et al.* 2020). As a major grain production base in China, the area of arable land, particularly rice fields, has expanded significantly in recent years. Moreover, under the future CC scenarios, the crop and irrigation requirements in this region will increase by 10%, indicating greater water consumption for agriculture. Changes in meteorological conditions,

particularly temperature and precipitation, have both direct and indirect impacts on the sustainable supply and quality of water resources. In addition, land-use changes, such as urbanization, agricultural expansion, and forest logging, impact soil erosion, runoff, and ecosystems. Therefore, a better understanding of the mechanisms by which climate and land-use changes affect hydrological processes in this basin is of great importance to scientists, policymakers, and watershed managers.

With the increasing impact of CC on water resources, the quantitative differentiation of its impact on runoff has attracted increasing attention. A series of uncertainties may be present in the study of the hydrological impacts of CC, including climate models, greenhouse gas emissions, hydrological model structures, downscaling methods, and parameters. Based on the coupled watershed hydrological and terrestrial vegetation ecological models, the ecohydrological model can more accurately reflect the water–carbon exchange process of the land–atmosphere at the regional scale (Ji *et al.* 2021). As a physics-based semi-distributed continuous time-step hydrological model the Soil and Water Assessment Tool (SWAT) can be employed to model rainfall–runoff and predict the effects of land use and CC on water quality and hydrology in basins (Zhang *et al.* 2012; Lin *et al.* 2017).

Based on the distributed parameter approach, the SWAT model divides the basin into multiple subbasins and considers precipitation, evaporation, runoff, soil erosion, and water quality processes. The model simulates rainwater infiltration, runoff generation, evapotranspiration, soil erosion, and vegetation growth through time steps to generate hydrological data for the basin. The model includes a series of parameters such as soil, vegetation, meteorological, and topographic parameters. These parameters must be calibrated according to the characteristics of the study area to ensure that the model can accurately simulate hydrological processes. The SWAT model has been successfully applied in many regions worldwide and has been proven to fully reproduce the hydrological processes of watersheds spanning a range of geographical regions and climates. Anand *et al.* (2018) applied the SWAT model to study the spatiotemporal variations of irrigation regression water in the Ganga River Basin, India, and assessed the impact of human activities, such as irrigation, on the regional water balance, providing a valid decision basis for the planning and management of regional water resources.

CC and land-use change are often intertwined; however, there is currently a lack of comprehensive research on their complex interrelationships. Especially, the existing research has not fully explored the challenges and limitations that these models may encounter in their comprehensive application, especially in the context of studying the impact of CC and land-use change on ecological hydrological processes. It can be noted that there is currently limited research on the comprehensive application of these models and a lack of integrated analysis under specific research objectives. In addition, the existing literature on the impact of CC and land-use change on watershed hydrology usually focuses on the impact of a single or a few variables, and there is a less comprehensive evaluation of the interaction between multiple variables. This limitation may lead to an insufficient understanding of the combined impacts of CC and land-use change. For example, the interaction between precipitation and temperature changes caused by CC and land-use changes such as urbanization and agricultural expansion may complicate the prediction and understanding of hydrological impacts on watersheds. Furthermore, existing model application research often overlooks the impact of model parameter uncertainty on research results. The selection and adjustment of model parameters are crucial for the accuracy of simulation results, but research in this field is still insufficient. Especially in long-term hydrological simulations considering the impacts of CC and land-use change, parameter uncertainty may have a remarkable impact on the reliability of model predictions.

This study provides a comprehensive understanding of water resource management and ecological conservation in watersheds. This study aimed to fill the aforementioned research gaps and provide insights for the scientific community and policymakers to address the impacts of CC and land-use change on water resources and ecosystems in the Second Songhua River (SSR) basin. Through research on the response of the SSR basin to hydrology and water resources in a changing environment, the change characteristics of the hydrometeorological elements of this basin from 1975 to 2020 were revealed. Subsequently, the hydrological change process and causes in the basin were analyzed more accurately. First, the general situation of the SSR basin was illustrated; second, using the years of historical meteorological data in this basin, the historical change characteristics of hydrometeorological elements in the study area were explored. Finally, the principle, construction, and structure of the SWAT model are stated and used to analyze the runoff of the SSR basin. Furthermore, changes in hydrological elements in the basin under different land-use scenarios were explored, and the responses of hydrological processes to different land-use patterns were studied. This study is expected to provide practical value for realizing sustainable utilization of water resources in the Songhua River Basin. The innovation of this study is that it focuses not only on CC but also on the impact of land-use change on water resources, particularly at high latitudes. This comprehensive analysis considered the

combined effects of climate and land-use factors on hydrological processes and revealed the complex interactions between them, providing profound insights into the field of research.

2. RUNOFF OF THE SSR BASIN BASED ON THE SWAT MODEL

2.1. The overall overview of the SSR basin

The Songhua River Basin (Figure 1) is located in northeast China (119° 52′–132 ° 31′ E, 41° 42′–51° 38′ N). It is one of seven major watersheds in China, with a gross area of 556,800 km^2 (Faiz *et al.* 2018; Kumar *et al.* 2023a, 2023b; Sharma *et al.* 2023). The mainstream of the Songhua River is composed of three subbasins: the Nenjiang River Basin in the west, the upper Songhua River Basin in the south (SSR), and the lower Songhua River Basin in the northeast. The tributary of the Nenjiang originates from the Yile'huli mountains in the Greater Khingan, stretching from northwest to southeast, with an overall length of 1,370 km and a drainage area of 297,000 km. The SSR begins at Tianchi in the Changbai Mountains, with an entire length of 958 km, and flows through a land area of 73,400 km^2 from the southeast to the northwest. Downstream of the Songhua River, there is a wide river channel and gentle slope. It gathers water from the Nenjiang River and SSR and runs 939 km northeast before emptying into the Amur River (Faiz *et al.* 2020; Li *et al.* 2020; Su *et al.* 2021).

The SSR basin, located in the northeast China plain between 124° 62′–128° 8′ E and 41° 75′–45° 4′ N, flows through 26 counties of Jilin Province (Wang *et al.* 2018). A digital elevation map with a resolution of 90 m showed a basin elevation

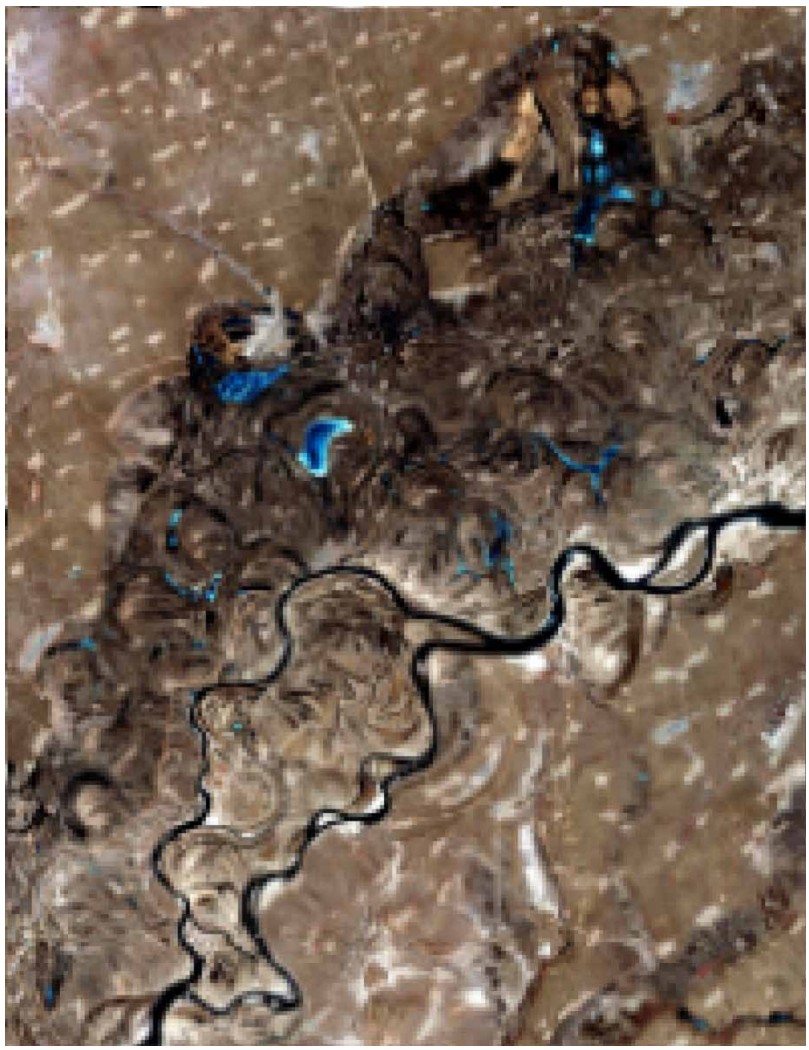

Figure 1 | Schematic diagram of Songhua River Basin (photograph credit: Wikipedia).

ranging from 121 to 2,729 m, decreasing from southeast to northwest. The basin is chiefly covered by black soil and has become one of the principal food-producing regions in China. To date, many valleys and plateaus have been cultivated in the Changbai Mountains. The land-use types in the basin are mainly forest and farmland, with rice as the main crop. The region has a mid-latitude monsoon climate with decreasing precipitation from southeast to northwest. Precipitation occurs mainly in summer and is accompanied by high temperatures (Wanhong *et al.* 2020). According to long-term historical data, the annual average precipitation is 400–600 mm, of which 70% occurs from June to September. From late November to early March, the average daily temperature is below the freezing point. According to the statistical data from the hydrology station at the downstream outlet, the measured monthly average discharge from July to September was greater than 500 m^3/s (Cui *et al.* 2020).

As observed through a quantitative evaluation of meteorological disasters from 1975 to 2008, the impact of drought on agricultural production has become increasingly serious over time (Zheng *et al.* 2016; Mohammed *et al.* 2022). As a result, many crops in the basin are highly sensitive to CC. The mean annual temperature (MAT) in northeast China has shown a significant upward trend, and over the last 40 years, the MAT in the region has been higher than the global and national averages. In Jilin Province, the influence of drought on agriculture is greater than the combined impact of flooding, hail, and low temperatures, and the severity of drought impact is increasing. As a major ecological agricultural area with black soil at high latitudes in the northeast China, it is important to explore the impact of CC on water resources in this region to provide information for promoting soil hydrology and ecological protection.

2.2. Study area and data collection

Precipitation is one of the most vital links in the water cycle, and the analysis of precipitation characteristics is conducive to understanding changes in water resources in a basin. Daily temperature and precipitation records from 37 meteorological stations were gathered from January 1975 to January 2020, and the annual rainfall and MAT were calculated. A Thiessen polygon was used to calculate the mean watershed precipitation.

The meteorological data were collected from meteorological observation stations, the geographic information data were mainly from Geographic Information System (GIS) databases, and the runoff observation data were from hydrological observation stations.

2.3. The structure and principle of the SWAT model

The SWAT model was developed by the Agricultural Research Center of the United States Department of Agriculture in 1994 (Lee *et al.* 2018; Basso *et al.* 2020; Zhang *et al.* 2020). At the hydrological response unit (HRU) level, the model calculates hydrological processes occurring in a basin, such as river flow, nutrient migration, sediment migration, and runoff. The HRU is a simple and unique combination of slopes within a subbasin, given the agrotypes and land cover types (Sahoo & Sahoo 2020). Structurally, each subbasin consists of at least one HRU, one tributary channel (used to calculate the confluence time of the subbasin), and one main channel. The HRU is the aggregate of the land surface area with the same vegetation cover, soil type, and management conditions in the subcatchments. The model utilizes land use, spatially distributed terrain, soil, and climate data as inputs and simulates sediment, pesticide, water, nutrients, and bacterial yield as outputs (Gong *et al.* 2019; Osei *et al.* 2019). The SWAT model is a simulation of the water and material cycles within a basin, which can be divided into two stages: land flow generation and water confluence of the water cycle. The integrated application structures of the SWAT model and GIS are shown in Figure 2.

The representation of the land part of the hydrological cycle in the SWAT model was based on the water balance equation (Equation (1)):

$$\mathrm{SW}_1 = \mathrm{SW}_0 + \sum_{i=1}^{t} (P_{\mathrm{day}} - Q_{\mathrm{surf}} - E_a - W_{\mathrm{seep}} - Q_{\mathrm{gw}}) \tag{1}$$

SW_0 and SW_1 are the initial and final water contents of the soil (mm), respectively; t represents the time step (d); Q_{surf} and Q_{gw} represent surface and underground runoff on the ith day (mm), respectively; E_a and P_{day} are the evapotranspiration and precipitation on the ith day (mm), respectively; and W_{seep} refers to the soil infiltration and lateral flow on the ith day (mm).

The complete process of the SWAT model in ArcGIS includes six steps. (1) data preparation; (2) construction of the SWAT model ArcSWAT; (3) initial run of the SWAT model ArcSWAT; (4) run of the SWAT model to simulate the hydrological

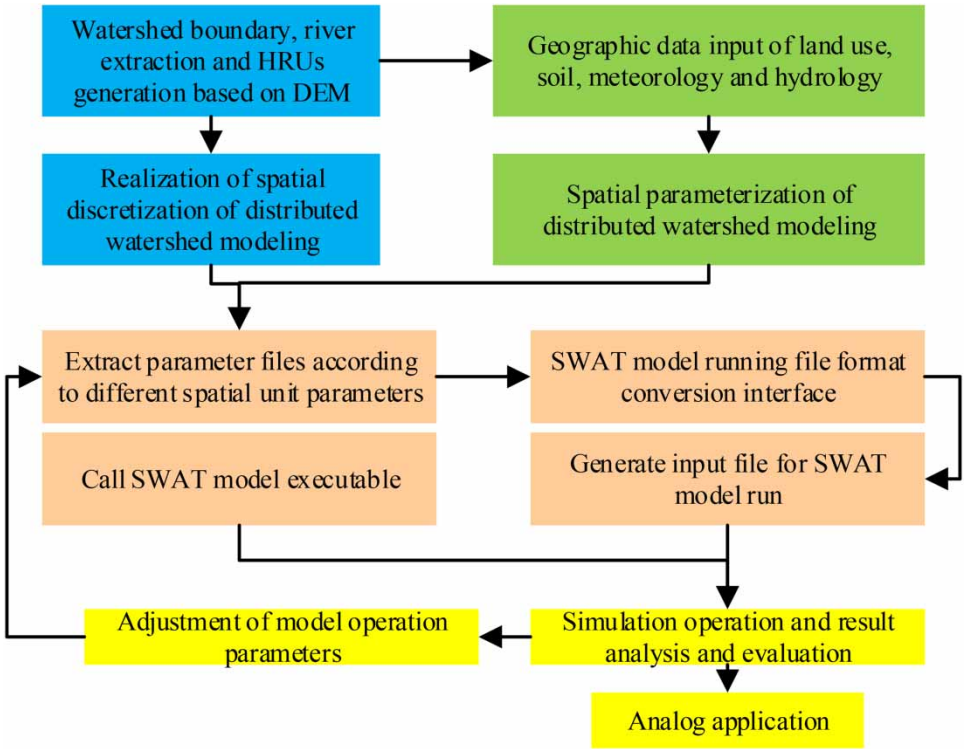

Figure 2 | Structure of the integrated application of SWAT model and GIS.

process; (5) use of ArcGIS tools to generate reports, charts, and maps to visualize and convey the model simulation results; and (6) statistics and analysis of simulation results. Hydrometeorological parameter calibration and validation of the model were used to adjust the relevant parameters in the model to ensure the model output sufficiently matched the observed data. For hydrometeorological parameters, this may include adjusting the meteorological parameters in the model (e.g., evapotranspiration coefficient, rainfall–runoff parameters) to ensure consistency of the simulated meteorological data as with the observed data. After calibration, the model was verified. In the validation phase, a separate dataset (as opposed to a calibration dataset) was used to evaluate the model performance. This can involve data that differ from the calibration data for the period and location in which the model was run to assess its generality and accuracy.

2.4. Construction of SWAT model in the basin

The ArcSWAT extension for SWAT version 2009 was employed to establish the model and simulate the data. The ArcSWAT basin tracer was adopted to map the watersheds into slopes, sub-watersheds, and drainage areas. The basin was subdivided into several HRUs with land-use categories, unique soil, and slope as input data. The input information for each sub-watershed was grouped into unique land cover areas, soil, weather categories, and management within the sub-watershed. Considering the impact of multiple physical processes on hydrology, the loading and movement of runoff, nutrients, sediment, and pesticides in the main river channel in each subbasin were simulated. Based on the steps shown in Figure 3, weather data are used for the calibration and validation processes. Model performance statistics were assessed, and water availability within the catchment was evaluated based on water balance ratios.

In this study, digital elevation model (DEM) data, soil attributes, land utilization, precipitation, temperature, and other meteorological data for the SSR basin were collected to create a SWAT model database. In addition, long-term historical runoff data were used to calibrate and determine the model parameters, and A SWAT model suitable for the hydrological simulation of the basin was implemented. The DEM was derived from the global terrestrial DEM established by the United States Geological Survey (USGS), using the WGS84 datum with a horizontal resolution of 30 arcsec (Pavri & Farrell 2020). Figure 4 shows the altitude data from the NASA radar observations of the space shuttle Endeavor. Soil attribute data were obtained from the Scientific Data Center in Cold and Arid Regions, and the data source was 1:1,000,000 soil data

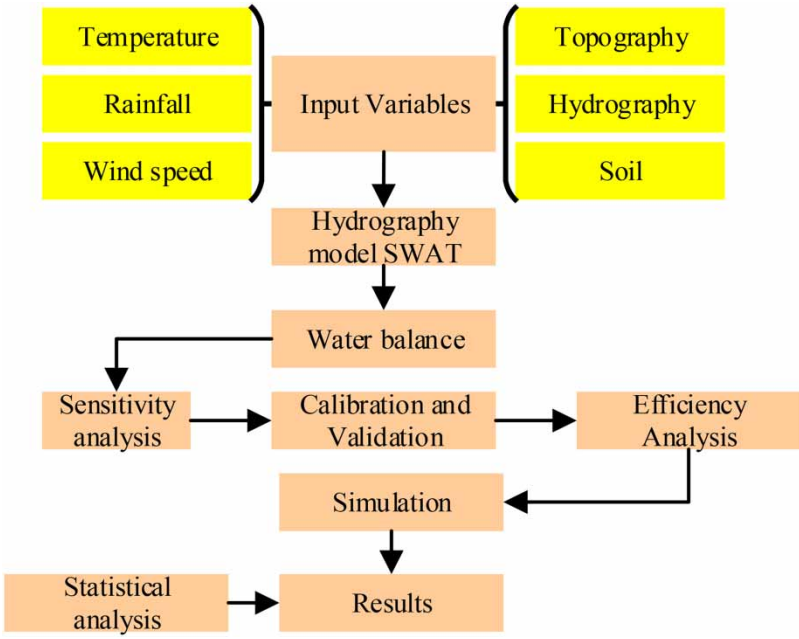

Figure 3 | Hydrological processes of the SWAT model.

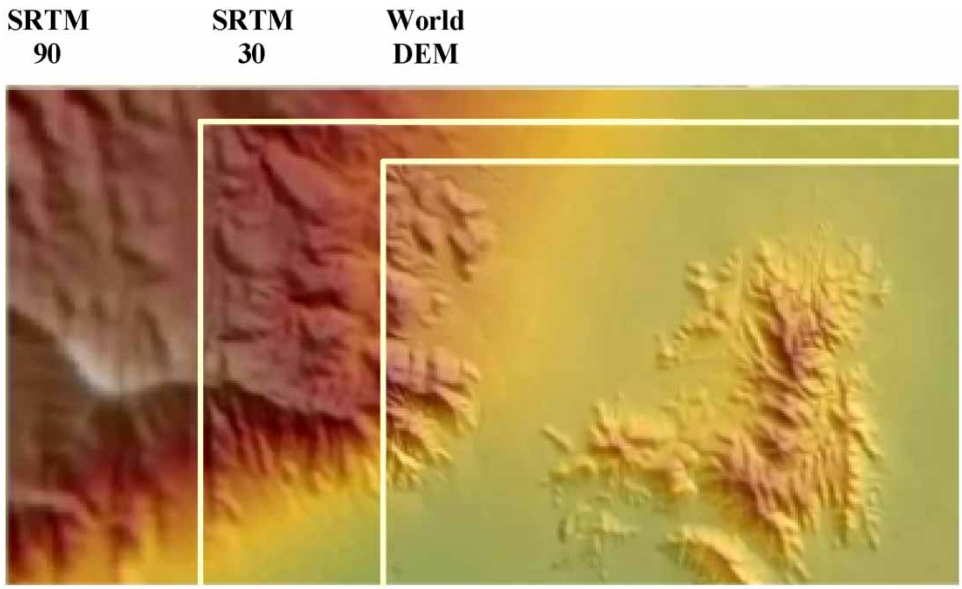

Figure 4 | Hydrological processes of the SWAT model.

provided by the Institute of Soil Science (ISS) in the second National Land Survey. Land-use data were collected from the National Earth System Science Data Center and included five types: cultivated land, forest land, urban residential land, grassland, and unused land. Weather data were obtained from the China Meteorological Data Sharing Service System, covering the daily mean values of 11 meteorological stations in the SSR basin. Hydrological data were obtained from the hydrographic stations in the Songhua River Basin, and Fuyu Station was selected as the SSR control station.

To implement the SWAT model, measured river flow data were required to demarcate the model parameters. Owing to the limitations of observational data, only observational river flow data from Fuyu Station, a hydrological survey station, were

used in this study. The data from the Fuyu Station can be employed to represent the hydrological processes of the entire basin; therefore, it is appropriate to use the data from the station for calibration. The model parameters were adjusted until the model results were similar to the behavior of the observed system. The correction process of the hydrological model can be expressed as follows:

$$Q(x, t) = M(\theta, x, t) + \varepsilon(x, t) \tag{2}$$

where $Q(x,t)$ implies the flow measured at point x and time t; $M(\theta,x,t)$ represents the estimated flow value obtained through a set of parametersθ; and $\varepsilon(x,t)$ displays the error at this point in the time interval.

Automatic and manual calibrations were performed and the parameters were appropriately changed to accommodate the observation information. Autocalibration was performed using Soil and Water Assessment Tool-Calibration and Uncertainty Procedures (SWAT-CUP), and the Sequential Uncertainty Fitting version 2 (SUFI-2) algorithm was adopted to readjust the parameters through multiple iterations to fit the observed values. Without changing any input parameter values, the calibrated model verification was used to compare the field observation data (data not used in the calibration) with the model prediction and then verify the calibrated model.

The current version of the SWAT model (SWAT-SuFI-2) covers several objective functions for evaluating performance. The Nash–Sutcliffe efficiency is a standardized statistic widely applied in deterministic and hydrological models, and can be written as follows:

$$\mathrm{NSE} = 1 - \left[\frac{\sum_{i=1}^{n} (Y_i^{\mathrm{obs}} - Y_i^{\mathrm{sim}})^2}{\sum_{i=1}^{n} (Y_i^{\mathrm{obs}} - Y_i^{\mathrm{mean}})^2} \right] \tag{3}$$

where Y^{obs} and Y^{sim} refer to the observed and simulated flow, respectively, and Y^{mean} represents the average of the observed data.

The coefficient of determination, R^2, describes the proportion of the total variance in the observed data that the model can explain, and the value range is 0–1. The larger the value is, the smaller the error variance. A value greater than 0.5 is considered acceptable. The expression of R^2 is as follows:

$$R^2 = \frac{\left[\sum_i (Q_{m,i} - \overline{Q_m})(Q_{s,i} - \overline{Q_s}) \right]}{\sum_i (Q_{m,i} - \overline{Q_m})^2 \sum_i (Q_{s,i} - \overline{Q_s})^2} \tag{4}$$

where m and s represent the measured and simulated values, respectively; Q signifies the variable (such as flow); and i refers to the ith simulated data. Q_m and Q_s represent two sets of data, natural runoff and measured runoff, respectively. $Q_{m,i}$ and $Q_{s,i}$ refer to the natural runoff and the measured runoff corresponding to the ith data point, respectively. $\overline{Q_m}$ and $\overline{Q_s}$ denote the mean of natural runoff and measured runoff, respectively.

In this study, the historical meteorological and hydrological data of the SSR basin derived from years of observation and records were used. CC scenario data, such as Representative Concentration Pathway (RCP) 4.5 and RCP 8.5, have also been applied to predict future climate conditions. A distributed hydrological model of the SSR basin was constructed, and a physics-based modeling method was adopted. The model considers the effects of climate, terrain, soil, and vegetation on the hydrological processes of the basin. The model was validated using historical data to ensure that it accurately simulated the hydrological processes in the basin. The Revised Universal Soil Loss Equation (RUSLE) module of the SWAT model was used to predict basin hydrological processes under different land-use scenarios. GIS software (such as ArcGIS and Environment for Visualizing Images (ENVI)) was employed to process and analyze spatial data, including topographic maps, land-use maps, and meteorological data.

3. RESULTS AND DISCUSSION

3.1. Historical change characteristics of hydrometeorological elements in the study area

The average precipitation in the SSR basin from 1975 to 2020 was 698.38 mm. Affected by the East Asian monsoon climate, the annual distribution of precipitation in the basin is extremely uneven and mainly concentrated in summer. The precipitation from June to August accounts for 55–70% of the rainfall, which is 277.32–615.25 mm. As the winter climate is cold and dry, the precipitation from November to February is less than 5% of the annual precipitation. The interannual variation in precipitation in the SSR basin from 1975 to 2020 was studied, and a linear regression analysis was conducted in the study area, as indicated in Figure 5. Overall, precipitation in this basin presented a downward trend and was more abundant during 1975–1985. The Mann–Kendall analysis of precipitation in different seasons and the entire year showed that precipitation in spring and winter tended to increase, whereas that in summer and autumn decreased. The test statistic of annual precipitation in this region is −0.834, exhibiting an insignificant downward trend. Table 1 presents the results of the study.

The three northeastern provinces have a monsoon climate at medium latitudes, but owing to the high latitudes of some regions, the winter is cold and long, and the summer is warm and short (Faiz *et al.* 2020; Gou *et al.* 2020; Cidan *et al.* 2022). The distribution of the temperature zone and wet and dry areas is as follows: most are in the middle temperate zone, a small part is in the cold and warm temperate zones, as well as a small part in the humid and subhumid zones. Northeast China spans middle and cold temperate zones from south to north. It has a temperate monsoon climate with four distinct

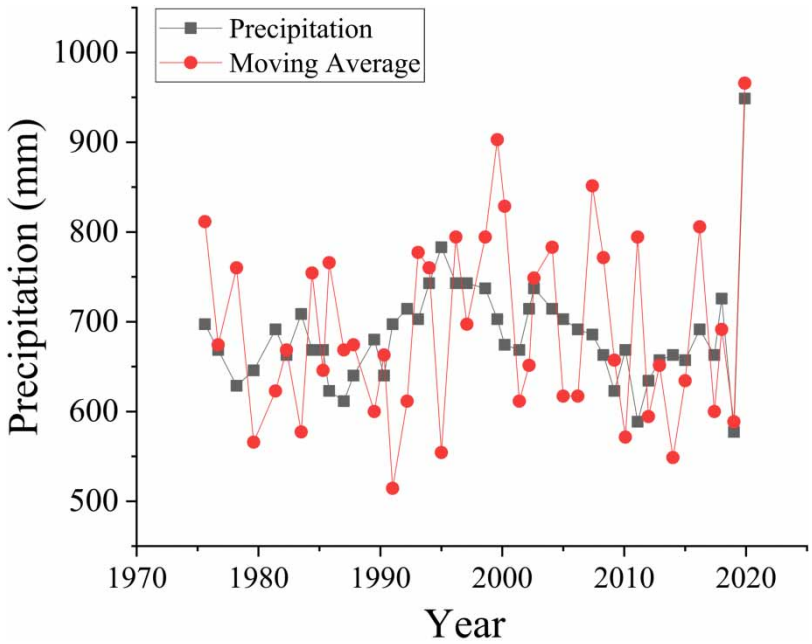

Figure 5 | Variation trend of precipitation in the SSR basin from 1975 to 2020.

Table 1 | Mann–Kendall analysis results of precipitation series in the SSR basin

Precipitation series	Test statistics	Precipitation trend
Spring	1.062	Increase
Summer	−0.515	Decrease
Autumn	−1.983	Decrease
Winter	0.125	Increase
Annual precipitation	−0.834	Decrease

seasons. It is rainy and warm in summer and dry and cold in winter. From southeast to northwest, annual precipitation drops from 1,000 mm to below 300 mm and transitions from humid and semi-humid areas to semi-arid regions. From 1975 to 2017, the average annual temperature (AAT) in northeast China rose at a rate of 0.31 °C/10 years, exceeding the national AAT in the same period and the global AAT in the recent 50 years. In contrast, the rising MAT rate in Liaoning Province was 0.27 °C/10 years.

The change in AAT in the SSR basin from 1975 to 2020 is shown in Figure 6. The MAT of the basin from 1975 to 2020 was 4.29 °C, and the MAT for spring, summer, autumn, and winter were 4.00, 20.11, 7.18, and −14.18 °C, respectively. The highest temperature was 21.29 °C in July, whereas the lowest was −16.61 °C in January. Figure 6 shows that the AAT of the SSR basin increases each year. The 5-year sliding average trend line indicates that the AAT variation in this region was small before 1985, with slight fluctuations and increases. The mean temperature of the basin continued to fluctuate and increased after 1991, after which it increased from 1986 to 1990. Overall, the AAT of the SSR basin maintained an increasing rate of 0.40 °C /10 years. Using the Mann–Kendall method for diverse seasons and AAT, it was found that the AAT test statistic of the basin was 5.53, showing a clear increase. The temperature in each season presented an increasing trend of varying degrees, and the rising trend in summer was relatively weak. Table 2 presents the results of the study.

The ArcGIS software was used to generate statistics on the area of land-use types at each stage, and the results are shown in Table 3. The data show that the area of land-use patterns in the SSR basin experienced little change, and the main trend is that

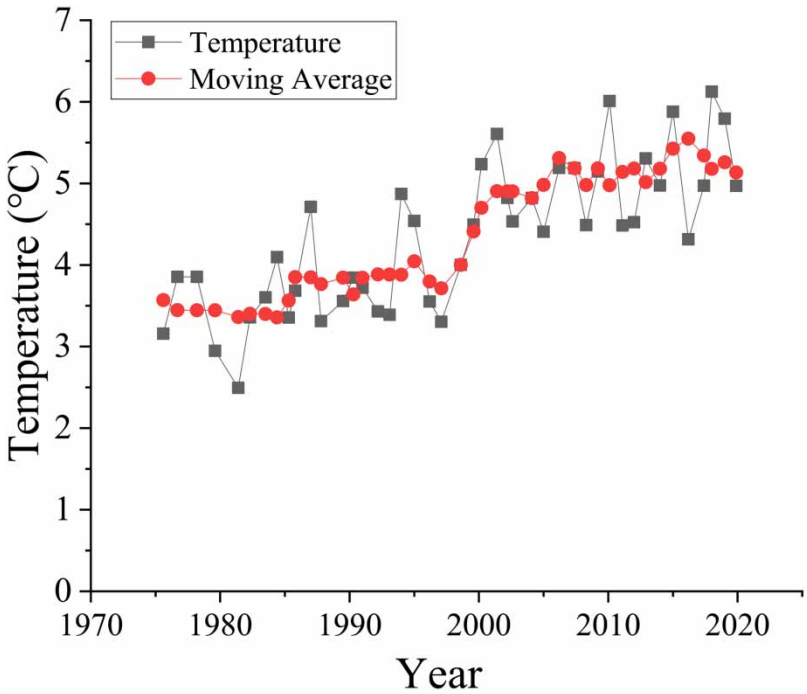

Figure 6 | Variation trend of AAT in the SSR basin from 1975 to 2020.

Table 2 | Mann–Kendall analysis results of temperature in the SSR basin

Temperature series	Test statistics	Temperature trend
Spring	4.45	Increase
Summer	2.53	Increase
Autumn	5.71	Increase
Winter	4.22	Increase
AAT	5.53	Increase

Table 3 | Changes in land-use patterns in the SSR basin (km^2)

Years	Cultivated land	Woodland	Grassland	Urban residential land	Unused land
1980	31,320	36,459	1,563	2,703	2,405
2000	31,828	36,153	1,485	2,792	2,194
2020	31,530	35,531	1,449	3,412	2,277

the area of woodland, grassland, and other unused land is decreasing, whereas the area of arable and urban residential land is increasing. Before 2000, land development and utilization in the basin involved cutting down and destroying woodland and grassland, developing unused land, and transforming it into agricultural and urban land.

Based on the runoff variation in the SSR basin collected by the Fuyu Hydrographic Station, the annual mean monthly runoff in the region was obtained; the results are shown in Figure 7. The annual average measured runoff in the study area was 468.75 m^3/s, and that of natural runoff was 510.42 m^3/s. Natural runoff is concentrated in July and August. Owing to the influence of artificial water intake, reservoir regulation, and storage, the annual process of the measured runoff was relatively stable. The Mann–Kendall analysis results for the natural runoff series in the SSR are shown in Table 4. The annual test statistics of the measured and natural runoff were −1.18 and −1.26, respectively, presenting an insignificant decreasing trend.

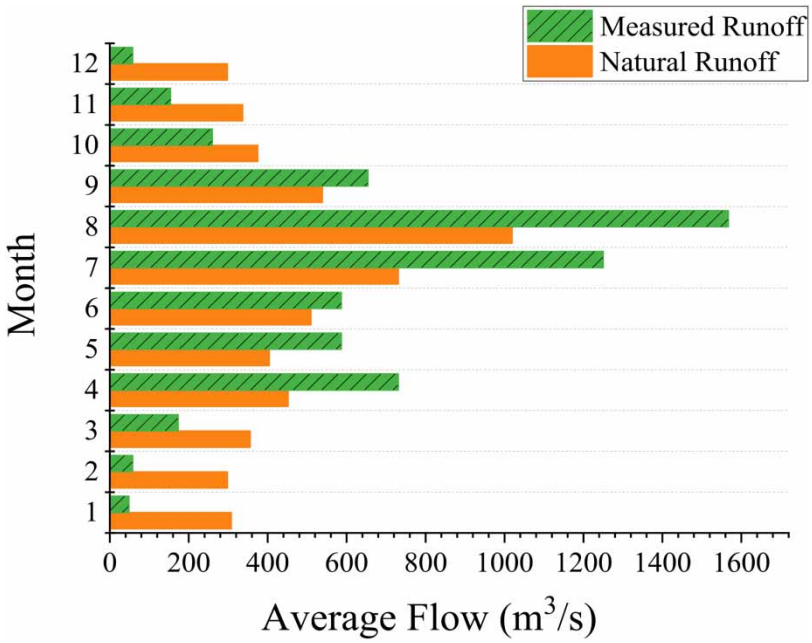

Figure 7 | Multi-year mean monthly runoff process in the SSR basin.

Table 4 | Mann–Kendall analysis results of natural runoff in the SSR basin

Natural runoff series	Test statistics of natural runoff	Test statistics of measured runoff	Trend (increase/decrease)
Spring	−1.11	−0.35	Decrease
Summer	−0.62	−1.73	Decrease
Autumn	−2.62	−0.75	Decrease
Winter	1.12	0.33	Increase
Annual runoff	−1.18	−1.26	Decrease

The Run-SWAT command was used to run the model and generate the simulation data required for this study. Here, the Daily rain/CN/Daily command was selected in the Rainfall/Runoff/Routing box to simulate runoff from January 1, 1975, to January 1, 2020. The Read SWAT OutPut command was used, the output file type on the right was selected, and Import Files to Database was clicked. The simulation results are saved in a project directory.

3.2. Runoff prediction under future CC

Over the late 21st century (2081–2100), under the low, moderate, and high emission scenario, the MAT in northeast China will likely rise by 1.2–2.0, 3.3–3.9, and 5.3–6.2 °C. During the base period (1975–2020), the MAT of the SSR basin was 4.2 °C. Under RCP 4.5, the MAT of the basin will increase by 5.4 °C from 2020 to 2049. Under CC scenarios RCP 4.5 and RCP 8.5, the temperature of the basin in June will increase by 0.2 and 1.1° C, respectively. The forecast trends of future CC in the basin are shown in Figure 8.

The constructed distributed hydrological model of the SSR basin was adopted to simulate and forecast the runoff of the basin from 2020 to 2049; the results are shown in Figure 9. Under RCP 4.5 and RCP 8.5, the mean annual flow of the basin will decline at an annual rate of 6.4 and 6.2 m^3/s.

3.3. Impact of land-use change on runoff

The land-use type changes in the study area were relatively small, and the area changes were all below 1,000 km^2, mainly due to the increase in cultivated and urban residential land areas and the decrease in woodland, grassland, and other unused land areas. Under the influence of human activities and CC, the vegetation leaf area index in the study area showed a significantly increasing trend from 1980 to 2010, with a slope of 0.28/10 years. Climate change not only has a direct impact on the water cycle but also affects the growth and succession of underlying vegetation, causing changes in factors such as surface sugar content and canopy impedance, indirectly affecting the surface water cycle.

During the 1980s and the 1990s, the area of construction land in the SSR basin increased by 410%, indicating that domestic and industrial water use increased significantly, making the conflict between water supply and demand even more pronounced. Based on the scenario prediction model method, this study combined the local natural economy, policy constraints, and other conditions to predict the future change trend of land and then simulated the hydrological response under the trend change. Six different land-use scenarios for the SSR basin were established. The baseline scenario was the land-use pattern in 2000. In scenarios 1 and 2, the land use was restored to 1975 and 1986, respectively. In scenarios 3, 4, and 5, all land-use types were woodland, grassland, and cultivated land, respectively. The ratios of basin types under diverse scenarios are listed in Table 5. Considering the trend of wetland degradation in the study area, we established three types of

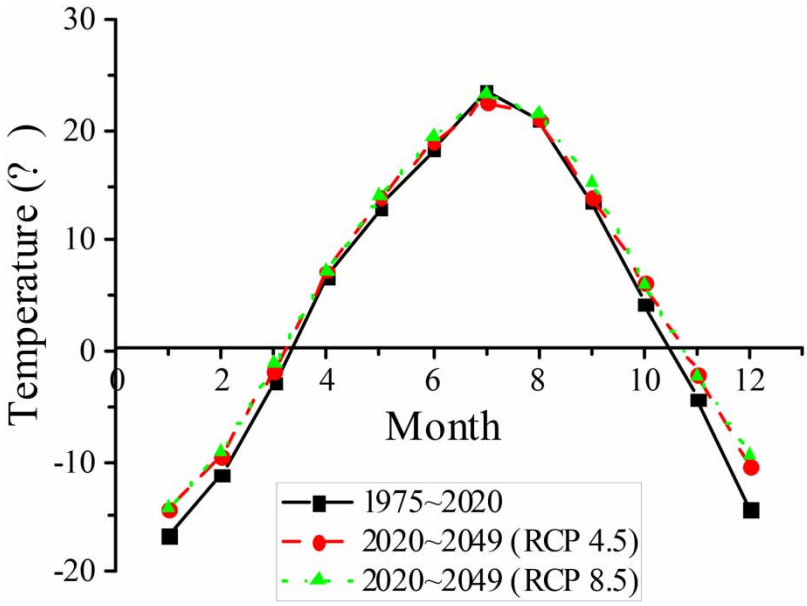

Figure 8 | Forecast of future CC trends in the SSR basin.

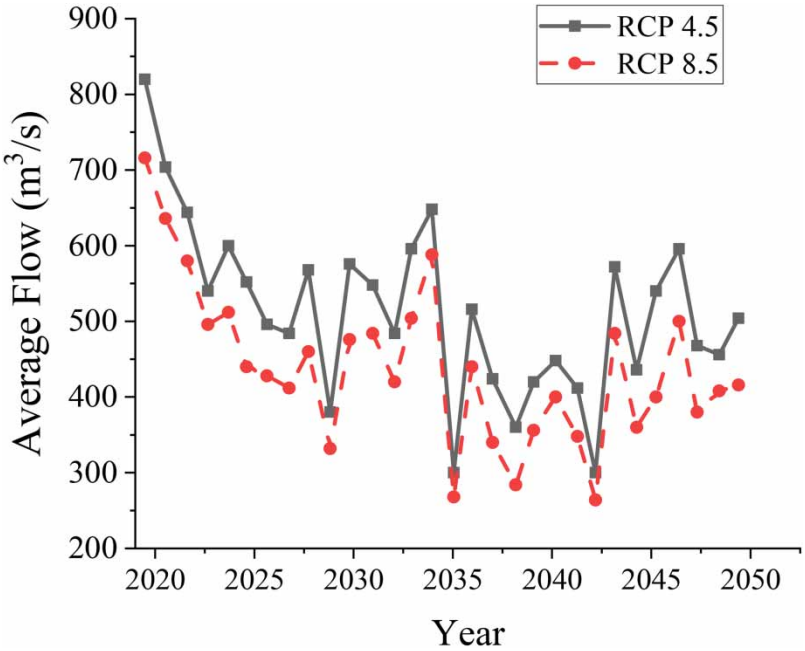

Figure 9 | Prediction of annual flow in the SSR basin.

Table 5 | Proportion of the main types of land use of six different land-use scenarios in the SSR basin

Scenario	Cultivated land/%	Woodland/%	Grassland/%	Total
Baseline scenario	39.7	13.6	39.1	92.4
Scenario 1	40.4	16.8	36.2	93.4
Scenario 2	38.5	21.2	32.6	92.3
Scenario 3	100	0	0	100
Scenario 4	0	100	0	100
Scenario 5	0	0	100	100

area-change scenarios for the construction of wetland change scenarios: the wetland area remained unchanged (wetland area*1) and decayed (wetland area*0.8, 0.5, and 0.3, respectively). In addition, for the water depth of the wetland, we considered three situations in which the depths of the wetlands were 0.5, 0.4, and 0.3 m. The wetland area and depth scenarios were combined to obtain 12 wetland change scenarios. Using various combinations of areas and water depths, the influence of wetland degradation on runoff was determined for the different scenarios. The simulation results of the annual average flow at the Fuyu Station (Table 6) showed that under different water depth conditions, the average flow in the basin gradually increased with a decrease in wetland area. When the initial area of the wetland was reduced by 0.8 times of the initial area, the average flow increase was approximately 14–15%.

Table 6 | Annual average flow under different wetland changes scenarios in the SSR basin

Average flow (m^3/s)	Wetland area*1	Wetland area*0.8	Wetland area*0.5	Wetland area*0.3
Water depth of wetland = 0.5 m	838.8	955.6	975.3	990.0
Water depth of wetland = 0.4 m	833.9	956.6	975.7	990.7
Water depth of wetland = 0.3 m	839.1	958.8	977.1	991.3

Note: The adjustment of wetland area and water depth is based on the land-use change module in the SWAT model.

3.4. Response analysis of runoff to CC

Natural runoff at the Fuyu Station was mainly concentrated in July and August. In addition, the runoff in April was relatively high because of the melting of winter snow, which formed spring floods. The annual measured runoff was relatively stable owing to the influence of artificial water intake and reservoir regulation. The trend analysis of runoff in different seasons reveals that the natural runoff at the Fuyu Station showed a remarkable downward trend in autumn, with a test statistic of −2.61. Runoff in winter showed an insignificant increasing trend. However, there was no prominent downward trend in spring or summer.

Based on the variations of temperature and precipitation in the SSR basin for RCP 4.5 and RCP 8.5, the mean temperature in the basin will increase by 0.9–1.6 °C, and precipitation will increase or decrease in various degrees in diverse regions. The SWAT hydrological model was employed to simulate the runoff of the basin under 25 CC scenarios (temperature changes of 0, 1, 2, −1, and −2 °C based on the annual average, and precipitation changes of 0, 10, 20, −10, and −20% of the original), and the corresponding monthly runoff of the basin was obtained. By comparing the simulation results of monthly runoff in the initial climate scenario, the percentage changes in the 25 CC scenarios relative to the initial climate scenario were obtained. The analysis results of the response of the mean monthly runoff in the SSR to the CC are shown in Figure 10. Runoff in the basin is negatively correlated with the temperature and positively related to precipitation. When the precipitation remained constant, the runoff decreased by 7.2% for a 1 °C temperature increase. When the temperature was constant, runoff increased by 30.5% for every 10% increase in precipitation. Under the 25 scenarios, the largest increase in runoff occurred when precipitation increased by 20% and temperature decreased by 2 °C, at which point the runoff increased by 75.1%.

Within a certain range, runoff is thought to be negatively correlated with temperature. This is because an increase in temperature may lead to increased evaporation, thereby increasing the soil water loss and reducing the surface runoff. However, the relationship between temperature and runoff may vary in different regions and seasons. For areas with ice and snow melt, an increase in temperature may lead to faster melting of ice and snow, thus increasing runoff.

3.5. Effectiveness and sensitivity analysis of SWAT model

The operation of the SWAT model involves numerous hydrological parameters, and the diversity and uncertainty of these parameters directly affect simulation results. In this case, we used SWAT-CUP software, based on the SUFI-2 algorithm,

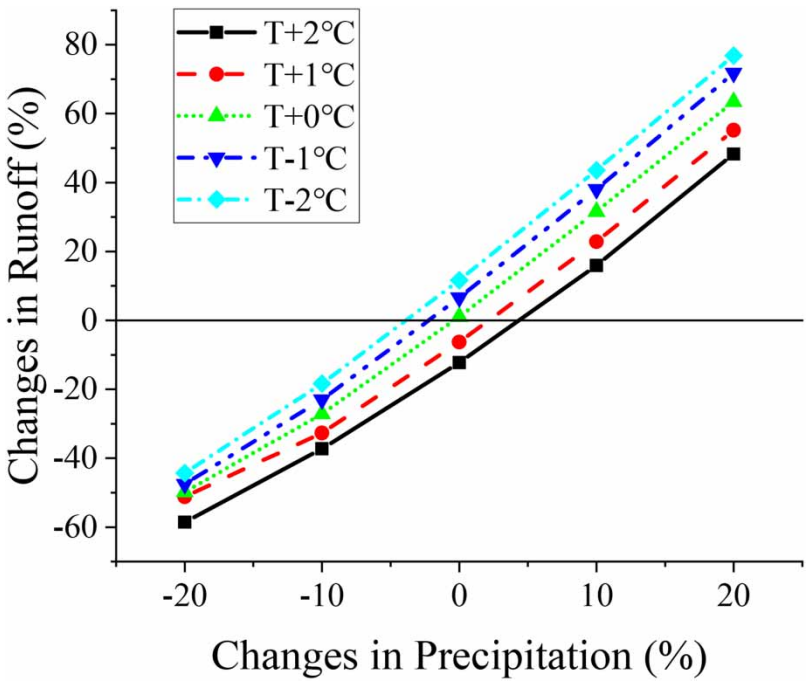

Figure 10 | Response of mean monthly runoff to CC in the SSR basin.

Table 7 | Runoff parameters and sensitivity analysis before and after modification of the SWAT model

Parameters	Means	Before modification		After modification	
		t-Stat	*P*-value	*t*-Stat	*P*-value
V__ESCO.hru	Groundwater evaporation coefficient	−1.00	0.30	−1.06	0.28
V__GW_DELAY.gw	Groundwater delay time	−0.88	0.37	−0.95	0.33
V__SURLAG.bsn	Lag coefficient of surface runoff	−0.80	0.42	−0.78	0.44
R__SOL_Z().sol	The depth from the surface layer of soil to the bottom layer of soil	0.69	0.49	0.70	0.48
V__GW_REVAP.gw	Coefficient of shallow groundwater re-evaporation	0.59	0.55	0.62	0.54

and global sensitivity analysis to perform a sensitivity analysis on the parameters of the watershed. In this study, t-Stat and *P*-values were used to verify the effectiveness of the SWAT model. We selected and compared the five parameters that were most sensitive to the runoff simulation. The results are presented in Table 7. The t-Stat value represents the sensitivity of the parameter, and the *P*-value reflects the significance of the t-Stat statistic. The greater the absolute value of t-Stat, the higher the sensitivity. The closer the *P*-value is to 0, the greater the significance. Compared with the parameters before modification, the absolute value of t-Stat of the runoff parameters of the modified model increased, whereas the *P*-value decreased, indicating that the sensitivity and significance of the modified model runoff parameters were improved.

4. DISCUSSION

In this study, the effects of climate and land-use change on runoff in the Songhua River Basin in northeast China were investigated using the SWAT model and multiple data sources. The simulation results showed that when precipitation remained constant, the annual runoff in the basin decreased by 7.2% for every 1 °C increase in temperature. This implies that as the temperature rises, water availability within the basin is threatened. Conversely, if the temperature remained the same but precipitation increased by 10%, the runoff increased by 30.5%. This highlights the complex interactions between temperature and precipitation, which are crucial for water resource management.

Another key discovery was the impact of land-use changes on runoff. This study simulated hydrological processes under different land-use scenarios and found that different land-use types play important roles in runoff generation. Astuti *et al.* (2019) confirmed this conclusion. Urbanization and agricultural expansion have significant impacts on the runoff of the basin. Urbanization can lead to changes in land area, reduced natural vegetation cover, and increased surface runoff. Conversely, agricultural expansion increases land erosion, leading to an increase in the sediment content of the runoff. These results suggest that land-use planning and management play critical roles in protecting basin water resources and ecosystems. This result is consistent with the findings of Li *et al.* (2021).

This study also highlighted the interactions between climate and land use. Under different climate scenarios, the effects of diverse land-use types on runoff may differ. For example, in RCP 4.5, the impact of urbanization on runoff likely increases significantly, whereas in RCP 8.5, agricultural expansion is likely to become a more dominant factor. This was confirmed by Ksenofontov & Polzikov (2020). This understanding of these interactions is critical for basin management and policy development, as it requires an integrated consideration of climate and land-use diversity to develop targeted measures.

The results of this study are of great significance for further understanding the mechanisms by which climate and land-use changes affect hydrological processes in the SSR basin. These results offer profound insights for the scientific community and provide a scientific basis for water resource management and ecological protection in this basin. In the face of future CC challenges, policymakers and watershed managers can take appropriate measures based on forecast information under various scenarios to ensure a sustainable water supply and protect ecosystem health. In addition, this study provides a comprehensive understanding of the hydrological processes related to changes in temperature and precipitation, which can help in future climate adaptation and sustainable development decision-making.

5. CONCLUSION

Considering that CC and land-use change are the main factors affecting runoff variation in the SSR basin, this study focused on analyzing their effects on ecohydrological processes. The variation of climatic elements in the study area was analyzed

based on the 45-year meteorological data series of the basin from 1975 to 2020. The SWAT model was used to predict hydrological processes under scenarios of land-use change and future CC. CC was found to be the main factor leading to a decrease in runoff in the basin from 1975 to 1989. The variations in land use in the basin were more evident during 1975–1986 and 1996–2000, and the runoff characteristics differed under the various scenarios. Wetlands play a role in regulating runoff, and the average flow increases gradually as the wetland area decreases. The results of the runoff simulation showed that the annual average flow of the Fuyu Hydrographic Station will decrease over the next 30 years, and the runoff will decrease gradually over the next 10 years. Owing to the limitations of ecohydrological simulations, this study has several shortcomings. In the future work, the influence of human activities on the ecohydrological evolution law should be considered to predict future water resource evolution in this basin more scientifically.

DATA AVAILABILITY STATEMENT

Data cannot be made publicly available; readers should contact the corresponding author for details.

CONFLICT OF INTEREST

The authors declare there is no conflict.

REFERENCES

Anache, J. A. A., Flanagan, D. C., Srivastava, A. & Wendland, E. C. 2018 Land use and climate change impacts on runoff and soil erosion at the hillslope scale in the Brazilian Cerrado. *Science of the Total Environment* **622–623**, 140–151.

Anand, J., Gosain, A. K. & Khosa, R. 2018 Prediction of land use changes based on land change modeler and attribution of changes in the water balance of Ganga Basin to land use change using the SWAT model. *Science of the Total Environment* **644**, 503–519.

Astuti, I. S., Sahoo, K. & Milewski, A. 2019 Impact of land use land cover (LULC) change on surface runoff in an increasingly urbanized tropical watershed. *Water Resources Management* **33**, 4087–4103.

Basso, M., Vieira, D. C. S., Ramos, T. B. & Mateus, M. 2020 Assessing the adequacy of SWAT model to simulate postfire effects on the watershed hydrological regime and water quality. *Land Degradation & Development* **31** (5), 619–631.

Berihun, M. L., Tsunekawa, A., Haregeweyn, N., Meshesha, D. T., Adgo, E., Tsubo, M., Masunaga, T., Fenta, A. A., Sultan, D., Yibeltal, M. & Ebabu, K. 2019 Hydrological responses to land use/land cover change and climate variability in contrasting agro-ecological environments of the Upper Blue Nile Basin, Ethiopia. *Science of the Total Environment* **689**, 347–365.

Cidan, Y. Z., Li, H. Y., Xuan, Y. Q., Sun, H. & You, F. 2022 Runoff forecast for the flood season based on physical factors and their effect process and its application in the Second Songhua River Basin, China. *Sustainability* **14** (17), 10627.

Cui, G., Su, X., Liu, Y. & Zheng, S. 2020 Effect of riverbed sediment flushing and clogging on river-water infiltration rate: A case study in the Second Songhua River, Northeast China. *Hydrogeology Journal* **29** (2), 551–565.

Faiz, M. A., Liu, D., Fu, Q., Uzair, M., Khan, M. I., Baig, F., Li, T. X. & Cui, S. 2018 Stream flow variability and drought severity in the Songhua River Basin, Northeast China. *Stochastic Environmental Research and Risk Assessment* **32** (5), 1225–1242.

Faiz, M. A., Liu, D., Fu, Q., Baig, F., Niaz, A. & Li, T. X. 2020 Effects of land use and climate variability on the main stream of the Songhua River Basin, Northeast China. *Hydrological Sciences Journal-Journal Des Sciences Hydrologiques* **65** (10), 1752–1765.

Gong, X. Y., Bian, J. M., Wang, Y., Jia, Z. & Wan, H. L. 2019 Evaluating and predicting the effects of land use changes on water quality using SWAT and CA-Markov models. *Water Resources Management* **33** (14), 4923–4938.

Gou, J., Miao, C. & Han, J. 2020 Spatiotemporal changes in temperature and precipitation over the Songhua River Basin between 1961 and 2014. *Global Ecology and Conservation* **24**, e01261.

Hu, S. S., Fan, Y. Y. & Zhang, T. 2020 Assessing the effect of land use change on surface runoff in a rapidly urbanized city: A case study of the central area of Beijing. *Land* **9** (1), 17.

Ji, G. X., Lai, Z. Z., Xia, H. B., Liu, H. & Wang, Z. 2021 Future runoff variation and flood disaster prediction of the Yellow River Basin based on CA-Markov and SWAT. *Land* **10** (4), 421.

Ksenofontov, M. Y. & Polzikov, D. A. 2020 On the issue of the impact of climate change on the development of Russian agriculture in the long term. *Studies on Russian Economic Development* **31**, 304–311.

Kumar, V., Azamathulla, H. M., Sharma, K. V., Mehta, D. J. & Maharaj, K. T. 2023a The state of the art in deep learning applications, challenges, and future prospects: A comprehensive review of flood forecasting and management. *Sustainability* **15** (13), 10543.

Kumar, V., Sharma, K. V., Caloiero, T., Mehta, D. J. & Singh, K. 2023b Comprehensive overview of flood modeling approaches: A review of recent advances. *Hydrology* **10** (7), 141.

Lee, S., Yeo, I. Y., Sadeghi, A. M., McCarty, G. W., Hively, W. D., Lang, M. W. & Sharifi, A. 2018 Comparative analyses of hydrological responses of two adjacent watersheds to climate variability and change using the SWAT model. *Hydrology and Earth System Sciences* **22** (1), 689–708.

Li, J., Dai, W., Sun, Y., Li, Y. H., Wang, G. Q. & Zhai, Y. Z. 2020 Different runoff patterns determined by stable isotopes and multi-time runoff responses to precipitation in a seasonal frost area: A case study in the Songhua River Basin, Northeast China. *Hydrology Research* **51** (5), 1009–1022.

Li, X., Yu, X. & Wu, K. 2021 Land-use zoning management to protecting the Regional Key Ecosystem Services: A case study in the city belt along the Chaobai River, China. *Science of the Total Environment* **762**, 143167.

Lin, F., Chen, X. W. & Yao, H. X. 2017 Evaluating the use of Nash-Sutcliffe efficiency coefficient in goodness-of-fit measures for daily runoff simulation with SWAT. *Journal of Hydrologic Engineering* **22** (11), 05017023.

Ma, Q. H., Zhang, K. L., Jabro, J. D., Ren, L. & Liu, H. Y. 2019 Freeze-thaw cycles effects on soil physical properties under different degraded conditions in Northeast China. *Environmental Earth Sciences* **78** (10), 321.

Mohammed, R., Zhang, Z. F., Hu, Y. H., Jiang, C., He, Z. Q., Wang, W. J. & Li, Y. F. 2022 Temporal-spatial variation, source forensics of PAHs and their derivatives in sediment from Songhua River, Northeastern China. *Environmental Geochemistry and Health* **44** (11), 4031–4043.

Osei, M. A., Amekudzi, L. K., Wemegah, D. D., Preko, K., Gyawu, E. S. & Obiri-Danso, K. 2019 The impact of climate and land-use changes on the hydrological processes of Owabi catchment from SWAT analysis. *Journal of Hydrology-Regional Studies* **25**, 100620.

Pavri, F. & Farrell, D. 2020 Arctic landscape transitions: Ice cap and terrestrial margins across Hofsjökull, Iceland. *Physical Geography* **42** (5), 472–488.

Sahoo, S. & Sahoo, B. 2020 Is hillslope-based catchment decomposition approach superior to hydrologic response unit (HRU) for stream-aquifer interaction modelling: Inference from two process-based coupled models. *Journal of Hydrology* **591**, 125588.

Sharma, K. V., Kumar, V., Singh, K. & Mehta, D. J. 2023 LANDSAT 8 LST pan sharpening using novel principal component based downscaling model. *Remote Sensing Applications: Society and Environment* **30**, 100963.

Su, L., Miao, C. & Gou, J. 2021 Long-term trends in Songhua River Basin streamflow and its multivariate relationships with meteorological factors. *Environmental Science and Pollution Research* **28** (45), 64206–64219.

Wang, M. Y., Lei, X. H., Liao, W. H. & Shang, Y. Z. 2018 Analysis of changes in flood regime using a distributed hydrological model: A case study in the Second Songhua River Basin, China. *International Journal of Water Resources Development* **34** (3), 386–404.

Wanhong, L., Fang, L., Fan, W., Maiqi, D. & Tiansen, L. 2020 Industrial water pollution and transboundary eco-compensation: Analyzing the case of Songhua River Basin, China. *Environmental Science and Pollution Research* **27** (28), 34746–34759.

Yan, Y., Zhen, H. C., Zhai, X. Y., Li, J. Y., Hu, W., Ding, C., Qi, Z., Qiao, B. L., Li, H., Liu, X. B. & Zhang, X. Y. 2021 The role of vegetation on earth bunds in mitigating soil erosion in Mollisols region of Northeast China. *CATENA* **196**, 104927.

Zhang, A. J., Zhang, C., Fu, G. B., Wang, B. D., Bao, Z. X. & Zheng, H. X. 2012 Assessments of impacts of climate change and human activities on runoff with SWAT for the Huifa River Basin, Northeast China. *Water Resources Management* **26** (8), 2199–2217.

Zhang, L. M., Meng, X. Y., Wang, H. & Yang, M. X. 2019a Simulated runoff and sediment yield responses to land-use change using the SWAT model in Northeast China. *Water* **11** (5), 915.

Zhang, Y., Wang, Y., Chen, Y., Liang, F. & Liu, H. 2019b Assessment of future flash flood inundations in coastal regions under climate change scenarios-a case study of Hadahe River Basin in Northeastern China. *Science of the Total Environment* **693**, 133550.

Zhang, H., Wang, B., Liu, D. L., Zhang, M. X., Leslie, L. M. & Yu, Q. 2020 Using an improved SWAT model to simulate hydrological responses to land use change: A case study of a catchment in tropical Australia. *Journal of Hydrology* **585**, 124822.

Zheng, L. Y., Yu, H. B. & Wang, Q. S. 2016 Application of multivariate statistical techniques in assessment of surface water quality in Second Songhua River Basin, China. *Journal of Central South University* **23** (5), 1040–1051.

Zhu, X. P., Zhang, A. R., Wu, P. L., Qi, W., Fu, G. T., Yue, G. T. & Liu, X. Q. 2019 Uncertainty impacts of climate change and downscaling methods on future runoff projections in the Biliu River Basin. *Water* **11** (10), 2130.

First received 6 August 2023; accepted in revised form 4 February 2024. Available online 27 February 2024